The Astrophysical Journal, 620:835–839, 2005 February 20

A POSSIBLE ORIGIN OF BIMODAL DISTRIBUTION OF GAMMA-RAY BURSTS

Kenji Toma,[1] Ryo Yamazaki,[2] and Takashi Nakamura[1]
Received 2004 June 30; accepted 2004 November 1

ABSTRACT

We study the distribution of the durations of gamma-ray bursts (GRBs) in the unified model of short and long GRBs recently proposed by Yamazaki, Ioka, and Nakamura. Monte Carlo simulations show clear bimodal distributions, with lognormal-like shapes for both short and long GRBs, in a power-law as well as a Gaussian angular distribution of the subjets. We find that the bimodality comes from the existence of the discrete emission regions (subjets or patchy shells) in the GRB jet. To explain other temporal properties of short and long GRBs, the subjet parameters should depend on the angle in the whole jet.

Subject headings: gamma rays: bursts — gamma rays: theory

1. INTRODUCTION

The durations of gamma-ray bursts (GRBs) observed by BATSE show a bimodal distribution, which has led to a classification of GRBs into two groups: bursts with T_{90} durations <2 s are called short GRBs, and those with durations >2 s are called long GRBs (Kouveliotou et al. 1993; McBreen et al. 1994). If T_{90} directly reflects the active time of the progenitor of the GRB, different origins of short and long bursts are implied, such that the former arise from binary neutron star mergers, while the latter arise from the collapse of massive stars (e.g., Mészáros 2002; Zhang & Mészáros 2004).

The short and long bursts roughly consist of 25% and 75%, respectively, of the total BATSE GRB population. We should regard these fractions as comparable, considering possible instrumental effects on the statistics. If these two phenomena arise from essentially different origins, the similar number of events is just by chance. However, some observations have suggested that the short GRBs are similar to the long GRBs (e.g., Germany et al. 2000; Lazzati et al. 2001; Nakar & Piran 2002; Lamb et al. 2003; Ghirlanda et al. 2004). Motivated by these facts, Yamazaki et al. (2004b) proposed a unified model of short and long GRBs, even including X-ray flashes (XRFs) and X-ray–rich GRBs, and showed that it is possible to attribute the apparent differences in the light curves and spectra of these four kinds of events to the different viewing angles of the same GRB jet. This is a counterargument against the current standard scenario of the origins of short and long GRBs.

In this paper, we perform Monte Carlo simulations to show that our unified model naturally leads the bimodal distribution of the T_{90} durations of GRBs. The paper is organized as follows. In § 2 we begin with a brief review of our unified model of short and long GRBs. The T_{90} duration distribution is calculated in § 3. Section 4 is devoted to discussions.

2. UNIFIED MODEL OF SHORT AND LONG GRBs

We briefly describe our unified model of short and long GRBs (for details, see Yamazaki et al. 2004b). We assume that the GRB jet is not uniform but made up of multiple subjets, and that each subjet causes a spike in the observed light curve. This is an extreme case of an inhomogeneous jet model (Nakamura 2000; Kumar & Piran 2000). Let us consider a subjet with the opening half-angle $\Delta\theta_{\rm sub}$ moving with Lorentz factor γ, observed from the viewing angle θ_v. Because of relativistic effects, the subjet emission becomes dim and soft when θ_v is larger than $\sim\Delta\theta_{\rm sub}+\gamma^{-1}$ (Ioka & Nakamura 2001). The *effective* angular size of its emission region is $\pi(\Delta\theta_{\rm sub}+\gamma^{-1})^2$, which is larger than the geometrical size of $\pi\Delta\theta_{\rm sub}^2$. For the multiple subjet case, the crucial parameter is the multiplicity (n_s) of the *effective* emission regions along a line of sight. If many subjets point toward us (i.e., $n_s \gg 1$) the event looks like a long GRB, while if a single subjet points toward us (i.e., $n_s = 1$) the event looks like a short GRB.

Below we give a typical set of parameters for the temporal and spatial configurations of the GRB jet to demonstrate which type of event is observed depending on n_s. We suppose that $N_{\rm tot}$ subjets are launched from the central engine of the GRB randomly in time and directions and that the whole jet consists of these subjets. We introduce a spherical coordinate system (r, ϑ, φ) in the central engine frame, where the origin is the location of the central engine, and $\vartheta = 0$ is the axis of the whole jet. The axis of the jth subjet ($j = 1, \cdots, N_{\rm tot}$) is denoted by $(\vartheta^{(j)}, \varphi^{(j)})$, while the direction of the observer is denoted by $(\vartheta_{\rm obs}, \varphi_{\rm obs})$. We suppose that the jth subjet departs at time $t_{\rm dep}^{(j)}$ from the central engine and emits at radius $r = r^{(j)}$ and time $t = t_{\rm dep}^{(j)} + r^{(j)}/\beta^{(j)}c$. The departure time of each subjet $t_{\rm dep}^{(j)}$ is assumed to be homogeneously random between $t = 0$ and $t = t_{\rm dur}$, where $t_{\rm dur}$ is the active time of the central engine measured in its own frame and is set to $t_{\rm dur} = 20$ s. The emission model for each subjet is the same as the uniform jet model in Yamazaki et al. (2003a). For simplicity, all the subjets are assumed to have the same intrinsic luminosity and opening half-angle $\Delta\theta_{\rm sub}^{(j)} = 0.02$ rad, and the other properties are $\gamma^{(j)} = 100$, $r^{(j)} = 3\times10^{13}$ cm, $\alpha_B^{(j)} = -1$, $\beta_B^{(j)} = -2.5$, and $\gamma h\nu_0'^{(j)} = 500$ keV for all j. The opening half-angle of the whole jet is set to $\Delta\theta_{\rm tot} = 0.3$ rad. We randomly spread $N_{\rm tot} = 350$ subjets following the angular distribution function of the subjets as

$$\frac{dN}{d\Omega} \equiv n(\vartheta,\varphi) = \begin{cases} n_c, & 0 < \vartheta < \vartheta_c, \\ n_c(\vartheta/\vartheta_c)^{-2}, & \vartheta_c < \vartheta < \vartheta_b, \end{cases} \quad (1)$$

where $\vartheta_b = \Delta\theta_{\rm tot} - \Delta\theta_{\rm sub}$, and $\vartheta_c = 0.02$ rad (see also Rossi et al. 2002; Zhang & Mészáros 2002). Figure 1 shows an

[1] Department of Physics, Kyoto University, Kyoto 606-8502, Japan; toma@tap.scphys.kyoto-u.ac.jp, takashi@tap.scphys.kyoto-u.ac.jp.
[2] Department of Earth and Space Science, Osaka University, Toyonaka 560-0043, Japan; ryo@vega.ess.sci.osaka-u.ac.jp.

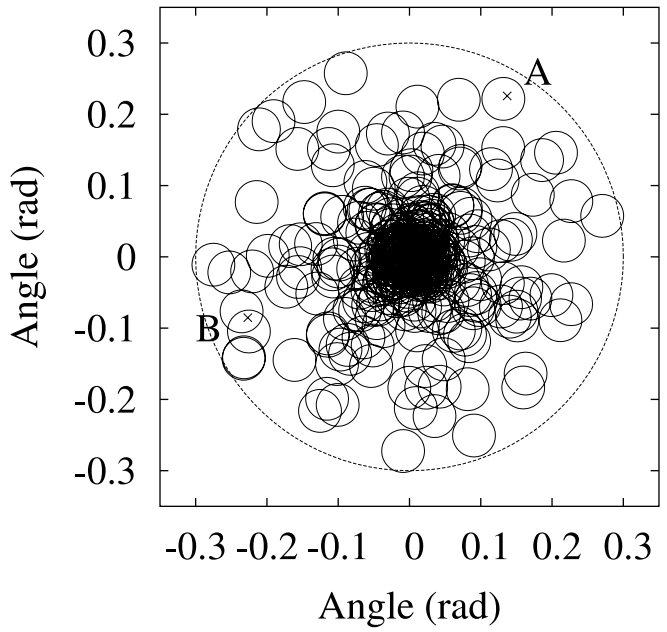

FIG. 1.—Angular distribution of $N_{\rm tot} = 350$ subjets confined in the whole GRB jet in our simulation. Each subjet is located according to the power-law distribution function of eq. (1). The whole jet has an opening half-angle of $\Delta\theta_{\rm tot} = 0.3$ rad. The subjets have the same intrinsic luminosity and opening half-angles $\Delta\theta_{\rm sub} = 0.02$ rad and the other properties of $\gamma = 100$, $r = 3\times10^{13}$ cm, $\alpha_B = -1$, $\beta_B = -2.5$, and $\gamma h\nu_0' = 500$ keV. The effective angular size of the subjets are represented by the solid circles, while the whole jet is represented by the dashed circle. The examples of lines of sight A and B are shown in the figure, while C is located at $(-0.04$ rad, 0.04 rad), and D is close to the center of the whole jet.

example of the angular distribution of the effective emission regions of the subjets in our calculation. Most of the subjets are concentrated near the $\vartheta = 0$ axis (i.e., the multiplicity in the center $n_s \sim 100$). For our adopted parameters, isolated subjets exist near the edge of the whole jet, and there are some directions in which no subjet is launched.

Figure 2 shows examples of the observed light curves in the 50–300 keV band, each of which corresponds to the lines of sight A, B, C, and D shown in Figure 1. The coordinate ($\vartheta_{\rm obs}$, $\varphi_{\rm obs}$) of C is $(-0.04$ rad, 0.04 rad), and D is close to the center of the whole jet. If many subjets point in the direction of our line of sight, such as in the cases of C ($n_s = 15$) and D ($n_s = 97$), we see a spiky temporal structure. In the case of B ($n_s = 2$), the event consists of the distinct emission episodes. These are identified as long GRBs. If only one subjet points toward us, like in the case of A ($n_s = 1$), the contributions to the observed light curve from the other subjets are negligible because of relativistic beaming effect, so that the observed gamma-ray fluence and duration are both about a hundredth of the typical values of long GRBs. These are quite similar to the characteristics of short GRBs. In addition, when the line of sight is away from any effective subjet regions (i.e., $n_s = 0$), the soft and dim prompt emission is observed because of relativistic Doppler effect and beaming effect, which is identified as an XRF or an X-ray–rich GRB. (Ioka & Nakamura 2001; Yamazaki et al. 2002, 2003a, 2003b, 2004a, 2004b).

3. DISTRIBUTION OF T_{90} DURATION

We perform Monte Carlo simulations to show that our unified model can explain the observed bimodal distribution of T_{90} durations of GRBs. We fix the subjets' configuration as in Figure 1. We vary only the line of sight of the observer and calculate the T_{90} duration for each observer in the 50–300 keV band. We generate 2000 lines of sight with $0 < \vartheta_{\rm obs} < 0.35$ rad according to the probability distribution of $\sin\vartheta_{\rm obs}\, d\vartheta_{\rm obs}\, d\varphi_{\rm obs}$. We then select only hard events, whose observed hardness ratio is $S(2-30\ {\rm keV})/S(30-400\ {\rm keV}) < 10^{-0.5}$ (Sakamoto et al. 2004). The other soft events are classified as XRFs or X-ray–rich GRBs, which are observed when all subjets are viewed off-axis.

Figure 3 shows the distribution of n_s in our simulation. The multiplicity n_s is roughly proportional to $n(\vartheta_{\rm obs}, \varphi_{\rm obs})$. Then the distribution of n_s is given by $P(n_s) \propto \sin(\vartheta_{\rm obs})(d\vartheta_{\rm obs}/dn_s) \sim n_s^{-2}$ (Fig. 3, *dashed line*). We first consider the T_{90} distribution in the case in which the redshifts of all the sources are fixed at $z = 1$ for simplicity. The result is shown in Figure 4. One can see a bimodal distribution of T_{90} clearly. Which type of burst is observed, long or short, depends on n_s, and the distribution of n_s is unimodal. Then why does the distribution of the duration become bimodal? The reason for the scarcity of the events for $1 < T_{90} < 10$ s is as follows. Let us first consider the event with $n_s = 1$. In this case the T_{90} duration does not vary significantly around $\sim$0.25 s when $\theta_v < \Delta\theta_{\rm sub}$, which is determined by the angular spreading time of a subjet. As the viewing angle increases, T_{90} increases (Ioka & Nakamura 2001). When $\theta_v \gtrsim \Delta\theta_{\rm sub} + \gamma^{-1}$, however, the emission becomes soft and dim, so that the event will not be detected as a GRB (Yamazaki et al. 2002, 2003a, 2003b). The T_{90} takes a maximum value of $\sim$0.75 s when $\theta_v \sim \Delta\theta_{\rm sub} + \gamma^{-1}$. We confirm that $n_s = 1$ for almost all $T_{90} < 1$ s events. Next let us consider the $n_s = 2$ case. The example of the light curve for this case is Figure 2*b*, and the T_{90} is 14.1 s. The T_{90} duration is roughly given by the interval between the arrival times of two pulses. Since the two pulses arrive sometime in the range $0 < T_{\rm obs} < T_{\rm dur}$, where $T_{\rm dur}$ is the active time of the central engine measured in the observer's frame, $T_{\rm dur} = (1+z)t_{\rm dur} = 40$ s, the mean interval is $40/3 = 13.3$ s. This means that the duration of the $n_s = 2$ event is much longer than that for $n_s = 1$. For $n_s \geq 3$, the mean duration is longer than 13.3 s. The typical example is Figure 2*c* for $n_s = 15$, with $T_{90} = 25.4$ s. This is the reason we have few events for $1 < T_{90} < 10$ s. The maximum value of T_{90} is $\sim T_{\rm dur}$. For the long bursts, the distribution function of T_{90} durations can be derived from a simple probability argument (see the Appendix for details). The dashed line in Figure 4 represents the analytical formula of equation (A2). On the other hand, the distribution function of the short bursts seems to be too complicated to calculate analytically, since it sensitively depends on the jet configurations, such as the angular distribution and the intrinsic properties of the subjets.

The ratio of events of the short GRBs and the long GRBs is about 2:5, which can be explained as follows (Yamazaki et al. 2004b). The event rate of the long GRBs is in proportion to the effective angular size of the central core $\vartheta_{c,{\rm eff}}^2 \sim (0.15\ {\rm rad})^2$, where $n_s \geq 2$. The event rate of the short GRBs is in proportion to $M(\Delta\theta_{\rm sub} + \gamma^{-1})^2$, where M is the number of isolated subjets in the envelope of the core, and $M \sim 10$ in our present case. Then the ratio of event rates of the short and long GRBs becomes $M(\Delta\theta_{\rm sub} + \gamma^{-1})^2 : \vartheta_{c,{\rm eff}}^2 \sim 2:5$.

In reality, we should take into account the source redshift distribution. We assume that the rate of GRBs is in proportion to the cosmic star formation rate. We adopt the model SF2 in Porciani & Madau (2001), in which we take the standard cosmological parameters of $\Omega_M = 0.3$ and $\Omega_\Lambda = 0.7$. Figure 5 shows the result. The distribution is again clearly bimodal, and the

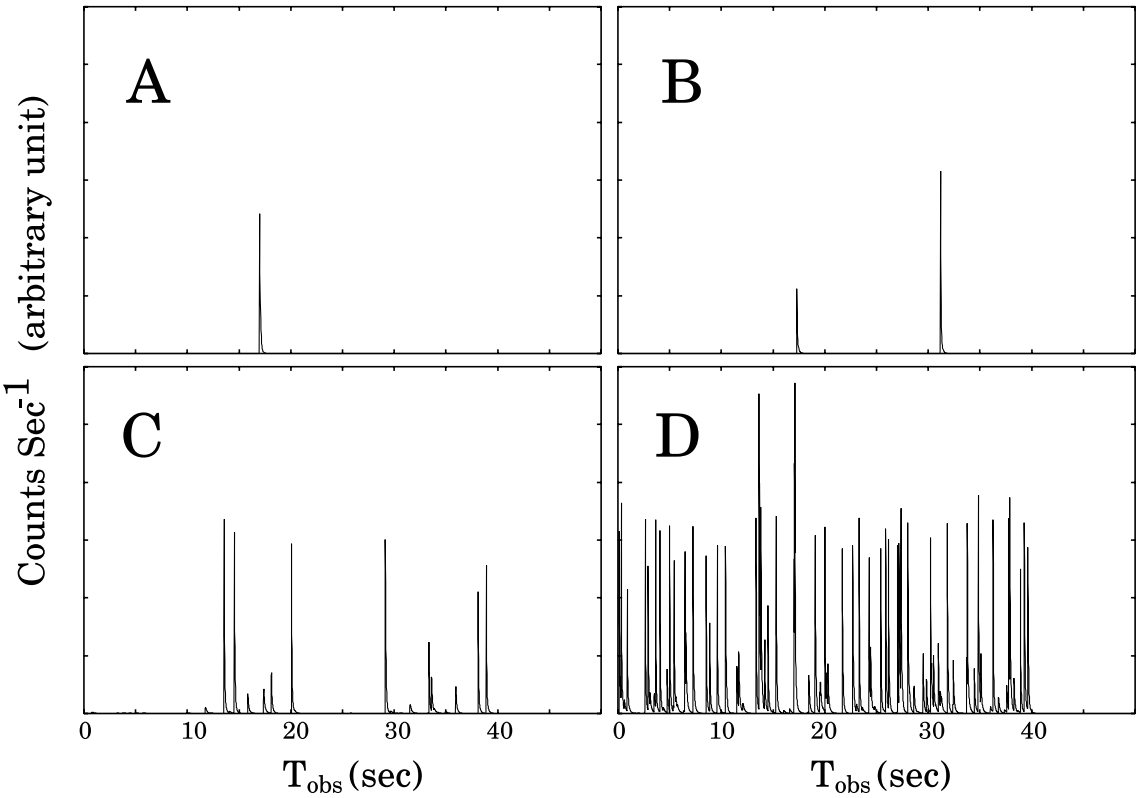

FIG. 2.—Observed light curves in the 50–300 keV band for the lines of sight shown in Fig. 1: A with $n_s = 1$ (*upper left*), B with $n_s = 2$ (*upper right*), C with $n_s = 15$ (*lower left*), and D with $n_s = 97$ (*lower right*). The sources are located at $z = 1$. The T_{90} durations are 0.25 s for A, 14.1 s for B, 25.4 s for C, and 37.8 s for D.

shapes of the short and long GRBs look like lognormal distributions. The ratio of the number of short and long GRBs is about 2:5 in this case as well. The dispersion of the lognormal-like distribution seems relatively small compared to the observations. This is ascribed to simple modeling in this paper. We fix the jet configuration and use the same intrinsic properties of the subjets. If we vary t_{dur} for each source and $\gamma^{(j)}$ for each subjet randomly, for example, the dispersion of lognormal-like T_{90} duration distribution will increase from the general argument that the dispersion of the lognormal distribution increases with the increase of the number of the associated random variables (Ioka & Nakamura 2002). In more realistic modeling, the observed dispersion will be reproduced.

4. DISCUSSION

We have investigated the T_{90} duration distribution of GRBs under the unified model of short and long GRBs proposed by Yamazaki et al. (2004b) and found that the model can reproduce the bimodal distribution observed by BATSE. In our model, the

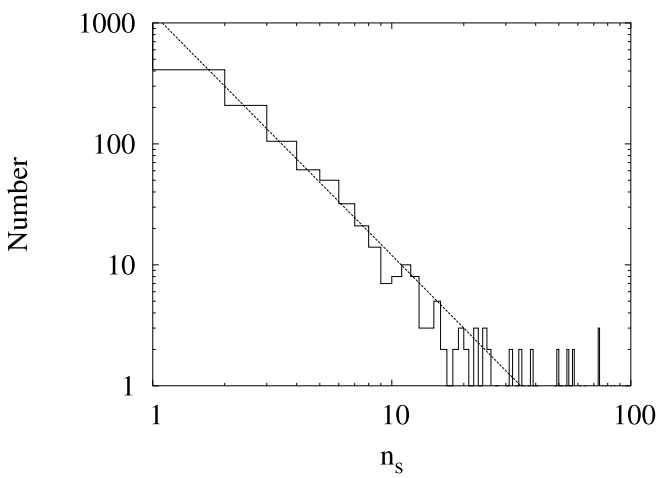

FIG. 3.—Distribution of multiplicity n_s for the angular distribution of the subjets of Fig. 1. The dashed line represents the analytical estimate of the n_s^{-2} line (see text).

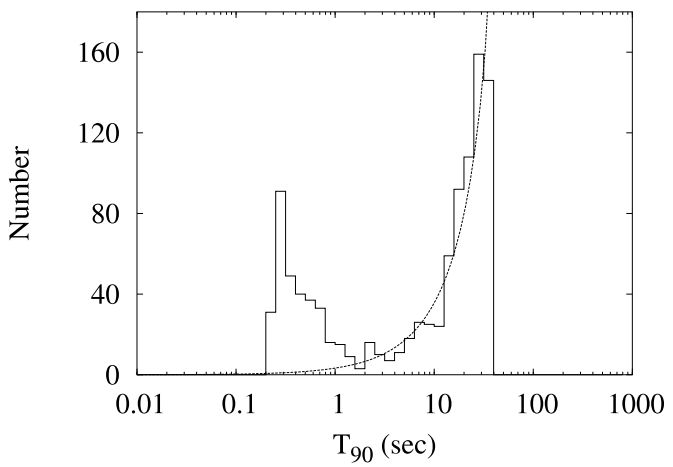

FIG. 4.—T_{90} duration distribution in the 50–300 keV band of hard events with observed fluence ratio $S(2-30\ \mathrm{keV})/S(30-400\ \mathrm{keV}) < 10^{-0.5}$. The jet model is the power law. All sources are located at $z = 1$. The dashed line represents the analytical formula for the long GRBs, given by eq. (A2).

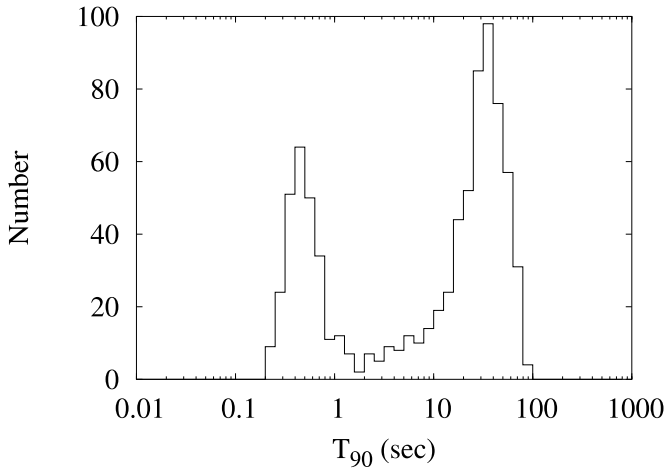

FIG. 5.—Same as Fig. 4, but the source redshifts are varied according to the cosmic star formation rate (see text for details). Both short and long GRBs look like lognormal distributions.

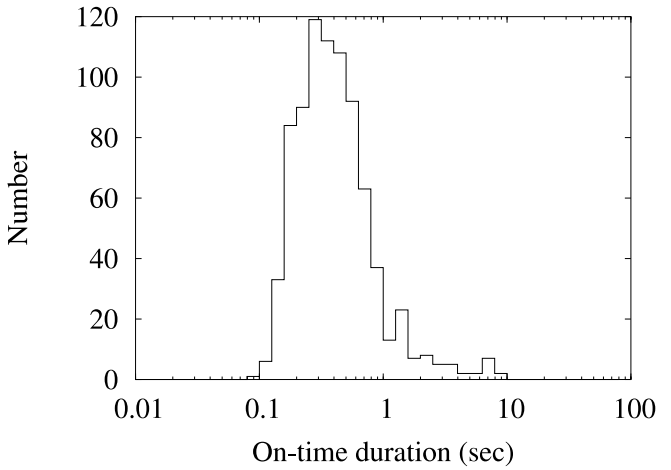

FIG. 6.—ON time duration distribution in the 50–300 keV band of hard events with observed fluence ratio $S(2-30\ \mathrm{keV})/S(30-400\ \mathrm{keV}) < 10^{-0.5}$. We calculate the ON time duration as the time during which the emission is larger than 10% of the peak flux. The subjet distribution is given by the power-law form. The source redshifts are varied according to the cosmic star formation rate.

crucial parameter is the multiplicity (n_s) of the subjets in the direction of the observer. The duration of an $n_s = 1$ burst is determined by the angular spreading time of one subjet emission, while that of an $n_s \geq 2$ burst is determined by the time interval between the observed first pulse and the last one. These two different time scales naturally lead a division of the burst T_{90} durations into the short and long ones. We also performed a similar calculation for a Gaussian distribution, $n(\vartheta, \varphi) = n_c \exp[-(\vartheta/\vartheta_c)^2/2]$, and found that the T_{90} duration distribution is bimodal in the same way as for the power-law subjet model.

Let us make another comparison of our model with BATSE data. Mitrofanov et al. (1998) have computed the distribution of the observed pulse number (denoted by n_p in their paper) and found that it is unimodal. If the n_p distribution were compared with the n_s distribution, our model might be compatible with the observations, although some long GRBs are identified as $n_p = 1$ events. They also derive the distribution of the ON time duration—defined as the time during which the emission is larger than 40% of the peak flux—and found it bimodal. Furthermore, they argue that the mean pulse widths of short and long GRBs are different. On the other hand, we computed the ON time duration distribution in the context of our theoretical model and found it unimodal (see Fig. 6), which is expected since the pulse widths are almost the same. However, there are several observational implications that the distances to short GRBs detected with BATSE are smaller than those of long GRBs (e.g., Tavani 1998; Ghirlanda et al. 2004), although this is controversial. Then the observed pulse widths for short and long GRBs might be different because of the redshift factor. To give an example, let us assume that the intrinsic luminosity of each subjet in the core region of the whole jet is larger than that in the periphery of the whole jet and count only the GRB events with peak flux larger than 3×10^{-4} of the maximum peak flux in our simulation. The result is shown in Figure 7, in which we find that the effect of the peak flux cutoff contributes to the bimodality of the ON time duration distribution.

At present, the observationally inferred bimodality of the ON time duration is not explained in our current model, in which all the subjets have the same intrinsic luminosity, the same opening half-angle, the same gamma factor, the same emission radius, and so on. This is an extreme modeling for simple calculation. In reality, they may depend on the off-axis angle in the whole jet; so may the pulse widths. Furthermore, Nakar & Piran (2002) investigated the pulse widths of GRBs using 2 ms time resolution and report that short GRBs also consist of several pulses. This can be incorporated into our model by assuming that a subjet radiates successive emissions rather than one instantaneous emission. Then the pulse width with 64 ms resolution (which is used in Mitrofanov et al. 1998) will be determined by the active time of the subjet. If the pulse widths from the subjets in the central part are larger than those in the periphery, the bimodality of the ON time duration distribution can be explained. For example, we assume that the emission radius $r^{(j)}$ is larger for the core region than for the periphery. Figure 8 is the result, which shows the bimodal-like distribution. Therefore, as we show in two examples (Figs. 7 and 8), some modifications of our model contribute to the bimodality of the ON time duration, so that the current observed ON time duration

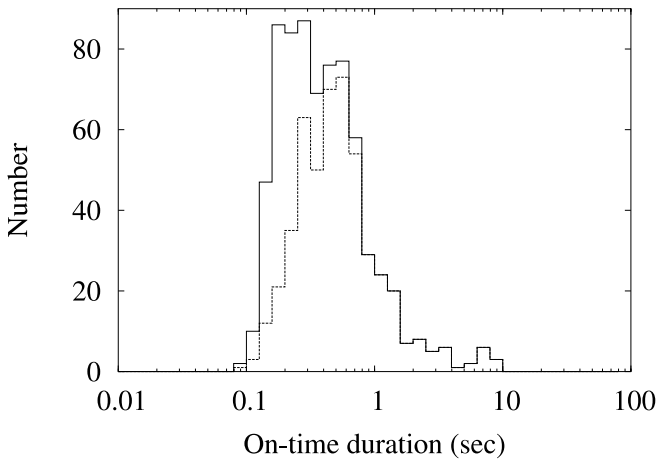

FIG. 7.—Same as Fig. 6, but the intrinsic luminosity of each subjet is assumed to be $A^{(j)} = A_0$ (= constant) for $\vartheta < 0.15$ rad and $A^{(j)} = A_0(\vartheta/0.15)^{-6}$ for 0.15 rad $< \vartheta < \vartheta_b$, where A_0 is in arbitrary unit. Then we only take the events with peak flux larger than 3×10^{-4} of the maximum peak flux that has appeared in the calculation. The dashed line represents $n_s \geq 2$ events.

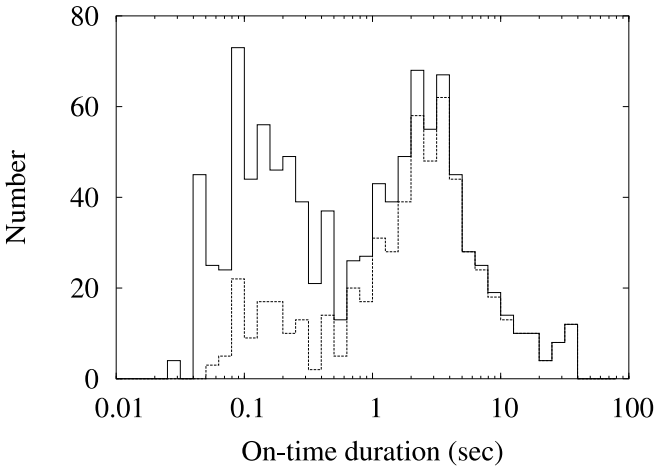

FIG. 8.—Same as Fig. 6, but the emission radius $r^{(j)}$ of each subjet is assumed to be $r^{(j)} = 3\times10^{14}$ cm for $\vartheta < 0.15$ rad and $r^{(j)} = 3\times10^{14}(\vartheta/0.15)^{-6}$ cm for 0.15 rad $< \vartheta < \vartheta_b$. The source redshifts are fixed as $z = 1$. The solid line represents all the events, while the dashed line represents $n_s \geq 2$ events.

distribution is not inconsistent with our model. We hope that in the future more sophisticated modeling will reproduce the observed ON time duration distribution.

It has commonly been said that the observed bimodal distribution of the T_{90} durations of BATSE bursts shows the different origins of short and long GRBs. However, the bimodal distribution is also available as a natural consequence of our unified model of short and long GRBs. The clear prediction of our unified model is that short GRBs are associated with energetic supernovae (SNe), since the association of long duration GRBs with SNe is strongly suggested (Galama et al. 1998; Stanek et al. 2003; Hjorth et al. 2003; Della Valle et al. 2003). Indeed, one of the short GRBs shows possible association with a SN (Germany et al. 2000). Even if the SNe are not identified with short GRBs because of some observational reasons, we predict that the spatial distribution of short GRBs in host galaxies should be similar to that of the long GRBs. Another prediction is that short GRBs have the same total kinetic energies as long GRBs, which might be confirmed by radio calorimetry (Berger et al. 2003).

We are grateful to the referee D. Lazzati for instructive comments. We would like to thank T. Piran for useful discussions. This work was supported in part by a Grant-in-Aid for the 21st Century COE "Center for Diversity and Universality in Physics" and also by Grants-in-Aid for Scientific Research of the Japanese Ministry of Education, Culture, Sports, Science, and Technology 05008 (R. Y.), 14047212 (T. N.), and 14204024 (T. N.).

APPENDIX

ANALYTICAL ESTIMATE OF THE INTRINSIC T_{90} DISTRIBUTION OF THE LONG BURSTS

In this Appendix we derive the analytical distribution function of the T_{90} durations of the long GRBs when all sources are assumed to be at $z = 1$. At first we consider for a given $n_s(\geq 2)$. Each subjet causes one pulse, whose shape is a δ-function for simplicity. In the present case, the arrival time of the pulse from each subjet is random in the range $0 < T_{\rm obs} < T_{\rm dur}$. For a given T_{90}, the first pulse is required to arrive within $T_{\rm dur} - T_{90}$. The arrival time of the last pulse is determined as the time T_{90} after the first pulse. The rest of the pulses are required to arrive within the range of T_{90}. Thus, the probability function of T_{90} for a fixed n_s is approximately given by

$$P_{n_s}(T_{90})\,dT_{90} = n_s(n_s-1)\frac{T_{\rm dur}-T_{90}}{T_{\rm dur}}\left(\frac{T_{90}}{T_{\rm dur}}\right)^{n_s-2}\frac{dT_{90}}{T_{\rm dur}}. \tag{A1}$$

For the power-law angular distribution of the subjets, the distribution function of n_s is proportional to n_s^{-2}, so that we get

$$P(T_{90})\,dT_{90} \propto \sum\nolimits_{n_s=2}^{\infty} n_s^{-2}P_{n_s}(T_{90})\,dT_{90} = \frac{(T_{90}/T_{\rm dur}) + [1-(T_{90}/T_{\rm dur})]\log[1-(T_{90}/T_{\rm dur})]}{T_{90}/T_{\rm dur}}\frac{dT_{90}}{T_{90}}. \tag{A2}$$

The distribution function of n_s for the Gaussian angular distribution of the subjets can be obtained in a similar way.

REFERENCES

Berger, E., et al. 2003, Nature, 426, 154
Della Valle, M., et al. 2003, A&A, 406, L33
Galama, T. J., et al. 1998, Nature, 395, 670
Germany, L. M., et al. 2000, ApJ, 533, 320
Ghirlanda, G., Ghisellini, G., & Celotti, A. 2004, A&A, 422, L55
Hjorth, J., et al. 2003, Nature, 423, 847
Ioka, K., & Nakamura, T. 2001, ApJ, 554, L163
———. 2002, ApJ, 570, L21
Kouveliotou, C., et al. 1993, ApJ, 413, L101
Kumar, P., & Piran, T. 2000, ApJ, 535, 152
Lamb, D. Q., et al. 2003, preprint (astro-ph/0312503)
Lazzati, D., Ramirez-Ruiz, E., & Ghisellini, G. 2001, A&A, 379, L39
McBreen, B., Hurley, K. J., Long, R., & Metcalfe, L. 1994, MNRAS, 271, 662
Mészáros, P. 2002, ARA&A, 40, 137
Mitrofanov, I. G., et al. 1998, ApJ, 504, 925
Nakamura, T. 2000, ApJ, 534, L159
Nakar, E., & Piran, T. 2002, MNRAS, 330, 920
Porciani, C., & Madau, P. 2001, ApJ, 548, 522
Rossi, E., Lazzati, D., & Rees, M. J. 2002, MNRAS, 332, 945
Sakamoto, T., et al. 2004, ApJ, 602, 875
Stanek, K. Z., et al. 2003, ApJ, 591, L17
Tavani, M. 1998, ApJ, 497, L21
Yamazaki, R., Ioka, K., & Nakamura, T. 2002, ApJ, 571, L31
———. 2003a, ApJ, 593, 941
———. 2004a, ApJ, 606, L33
———. 2004b, ApJ, 607, L103
Yamazaki, R., Yonetoku, D., & Nakamura, T. 2003b, ApJ, 594, L79
Zhang, B., & Mészáros, P. 2002, ApJ, 571, 876
———. 2004, Int. J. Mod. Phys. A, 19, 2385